SCIENCE CHINA
Information Sciences

• LETTER •

June 2023, Vol. 66 169403:1–169403:2
https://doi.org/10.1007/s11432-022-3537-1

Ultrahigh gain hot-electron tunneling transistor approaching the collection limit

Jun LIN[1,2†], Pengfei LUO[2†], Xinpei DUAN[2], Wujun ZHANG[2], Chao MA[2], Tong BU[2], Wanhan SU[2], Bei JIANG[1*], Guoli LI[2], Xuming ZOU[2], Ting YU[3], Lei LIAO[2*] & Xingqiang LIU[2*]

[1]*Faculty of Physics and Electronic Science, Hubei University, Wuhan* 430062*, China;*
[2]*State Key Laboratory for Chemo/Biosensing and Chemometrics, College of Semiconductors* (*College of Integrated Circuits*)*, Hunan University, Changsha* 410082*, China;*
[3]*School of Physics and Technology, Wuhan University, Wuhan* 430072*, China*

Received 16 January 2022/Revised 12 March 2022/Accepted 4 July 2022/Published online 4 April 2023

Citation Lin J, Luo P F, Duan X P, et al. Ultrahigh gain hot-electron tunneling transistor approaching the collection limit. Sci China Inf Sci, 2023, 66(6): 169403, https://doi.org/10.1007/s11432-022-3537-1

A hot-electron transistor (HET) is a unipolar and majority carrier device with voltage-controlled transport of ballistic hot electrons, and the monochromatic high-energy hot electrons are afforded by the tunnel and filter oxide barriers. The injected hot electrons from the emitter transit through the tunnel barrier with a width below the carrier mean free path (MFP) into the base region and then cross the filter barrier and are finally collected by the collector. A collection efficiency near unity is greatly desired for HETs to receive an ultrahigh current gain (β). As hot electrons quasi-ballistically traverse the base region, an ultra-short path for carrier transport below the MFP is needed [1]. Unfortunately, in traditional bulk HETs, thinning the base region increases its resistance and electrostatically decouples the collector from the emitter. The injected hot electrons are consequently thermalized by inelastic scattering, resulting in self-bias crowding.

Two-dimensional (2D) materials provide excellent electrical properties and an ultrathin body, promising ballistic transport of the carrier. However, previously reported 2D material-based HETs typically present low injection efficiency, which can be attributed to the challenge of efficiently modulating the height and width of the tunnel barrier (TB) and the filter barrier (FB). The chemically inert and hydrophobic surface of 2D materials does limit the conformal nucleation of an ultrathin dielectric layer with a high-quality interface. Therefore, relatively thick oxide layers (∼15–55 nm) have been used. Although many solutions for creating nucleation sites, such as an evaporated metal-oxide seed layer and plasma/ozone treatments [2], have been proposed to optimize the growth of oxide barrier layers, the involuntary introduction of impurities and defects results in degraded performance. Moreover, a 2D/3D heterojunction causes a large momentum difference between hot electrons before and after passing through the 2D/3D interface, where the hot electrons are intensively reflected [3–5]. Notably, a dielectric layer derived from 2D semiconductor materials can create an ideal interface for device fabrication. An ultrathin dielectric hafnium oxide (HfO_2) layer can be created by mild oxidation of hafnium disulfide (HfS_2) and is atomically flat [3]. The interface between HfS_2 and HfO_2 is atomically abrupt; thus, a uniform dielectric layer can be achieved without damaging adjacent HfS_2 layers. van der Waals integration can further offer an alternative bond-free interface with few traps. Owing to the introduction of a van der Waals heterojunction, all-2D-material-based HETs can reduce scattering and reflection of hot electrons, thereby improving hot-electron collection efficiency [6].

Herein, we demonstrate all-2D-material-based vertical HETs with an ultrahigh current gain and a collection factor approaching the collection limit at room temperature. The use of an atomically thin HfS_2 base and the in-situ growth of an ultrathin oxide barrier layer are found to greatly improve the injection efficiency of the emitter and reduce cold electron leakage. The HETs exhibit an ultrahigh β of 24104. The devices simultaneously present a high current density of 62 A/cm^2, a high on-off ratio over 10^5, and nanowatt power consumption at room temperature. The HETs developed in this study promise high potential for low-power, high-performance circuit design.

Experiment and measurement. Figure 1(a) is a schematic image of the fabricated HETs. The detailed fabrication processes are shown in Figure S1. Briefly, the HfO_2 TB and FB layers are formed by mild oxidation treatment of HfS_2 in air before and after the physical transfer process. Multilayer GeSe with a thickness of ∼30 nm serves as the contact electrode, which can reduce the scattering effect from the collector. Figure 1(b) is an optical image of the fabri-

* Corresponding author (email: jiangbei@whu.edu.cn, liaolei@whu.edu.cn, liuxq@hnu.edu.cn)
† Lin J and Luo P F have the same contribution to this work.

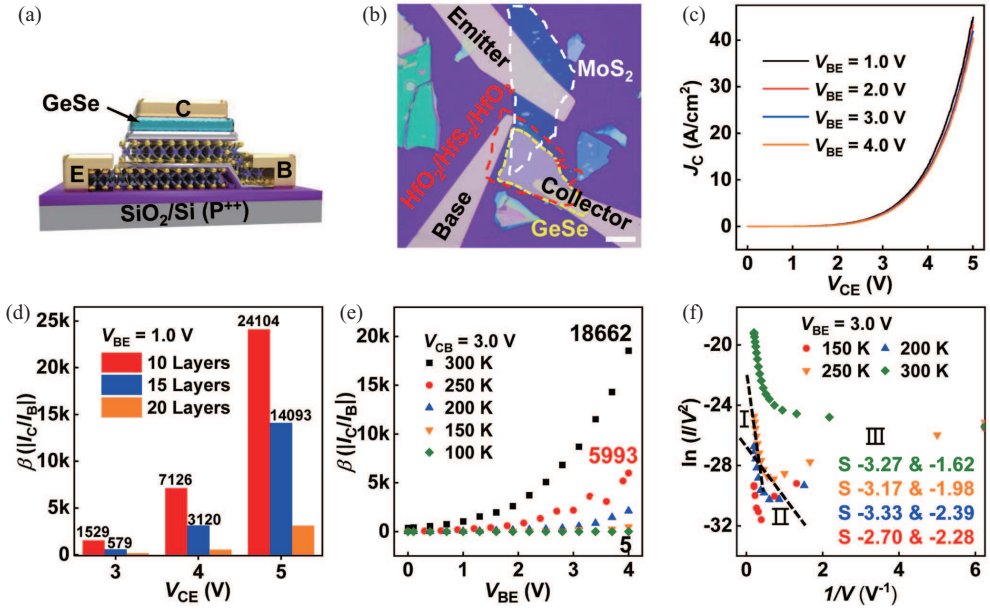

Figure 1 (Color online) (a) Schematic image of the hot-electron transistors (HETs). (b) Optical image of the HETs. The scale bar is 10 μm. (c) Typical output characteristics of the HETs. (d) Influence of the base-region thickness on α and β. (e) β versus $V_{\rm BE}$ at $V_{\rm CB} = 3.0$ V. (f) Fowler-Northeim plots at $V_{\rm BE} = 3.0$ V.

cated HETs. Figure S2 shows the cross-sectional transmission electron microscopy image as well as the distribution of the elements across the HETs, indicating atomic-thickness HfO_2 layers formed on both sides of HfS_2. The output characteristics of the HETs with different original HfS S_2 thicknesses are shown in Figure S3. As the thickness of the HfS_2 base is ten layers, the HETs obtain superior electrical performance, as shown in Figure 1(c). Because of the atomic thickness of the HfS_2 base region, hot electrons from the emitter can overcome barrier layers and directly contribute to $J_{\rm C}$. Figure 1(d) is the current gain (β) with a common emitter configuration. Scaling down the thickness of the base region below the MFP of a hot electron can promote the transition time and weaken the electrostatic decoupling of the collector and emitter. Therefore, a reduced HfS_2 base thickness affords large β values, and HETs obtain a record $\beta = 24104$ among the previously reported studies [7,8]. Figure 1(e) plots β values at different temperatures, and the detailed temperature-dependent electrical performance of the HETs with a common-based configuration is shown in Figure S4. Because hot electrons with high kinetic energy are conducive to improving the tunneling efficiency and probability, β increases with temperature accordingly. Transport mechanisms of hot electrons are identified by Fowler-Nordheim tunneling (FNT) plots [9]. Figure 1(f) shows FNT plots of $\ln(1/V^2)$ versus $1/V$ for the HETs. An entire FNT plot can be sectioned into three regions with different slopes corresponding to high (I), intermediate (II), and low (III) electric field regions, respectively. The slopes of the high and intermediate field regions are calculated from the least-squares fit to be between -4 and -1.5, which shows that FNT occurred in regions I and II for hot-electron transport while thermal emission dominates hot-electron transport in region III. A logarithmic regime (region III) for direct tunneling is presented at low temperature, which shows that carrier transport mechanisms transit from thermal emission at room temperature to direct tunneling at low temperature. This phenomenon is attributed to the hot electrons having insufficient kinetic energy to pass through barriers at low temperatures.

Acknowledgements This work was supported by National Key Research and Development Program of Ministry of Science and Technology (Grant No. 2018YFA0703700), China National Funds for Distinguished Young Scientists (Grant No. 61925403), China National Funds for Outstanding Young Scientists (Grant No. 62122024), National Natural Science Foundation of China (Grant Nos. 12174094, 51872084, 62004065, 62104065), and Natural Science Foundation of Hunan Province (Grant Nos. 2021JJ20028, 2020JJ1002).

Supporting information Figures S1–S4. The supporting information is available online at info.scichina.com and link.springer.com. The supporting materials are published as submitted, without typesetting or editing. The responsibility for scientific accuracy and content remains entirely with the authors.

References

1 Desai S B, Madhvapathy S R, Sachid A B, et al. MoS_2 transistors with 1-nanometer gate lengths. Science, 2016, 354: 99–102
2 Zou X, Wang J, Chiu C H, et al. Interface engineering for high-performance top-gated MoS_2 field-effect transistors. Adv Mater, 2014, 26: 6255–6261
3 Kümmell T, Hutten U, Heyer F, et al. Carrier transfer across a 2D-3D semiconductor heterointerface: the role of momentum mismatch. Phys Rev B, 2017, 95: 081304
4 Mleczko M J, Zhang C, Lee H R, et al. $HfSe_2$ and $ZrSe_2$: two-dimensional semiconductors with native high-κ oxides. Sci Adv, 2017, 3: e1700481
5 Zhu H, Wang J, Gong Z, et al. Interfacial charge transfer circumventing momentum mismatch at two-dimensional van der Waals heterojunctions. Nano Lett, 2017, 17: 3591–3598
6 Liang B W, Chang W H, Lin H Y, et al. High-frequency graphene base hot-electron transistor. ACS Nano, 2021, 15: 6756–6764
7 Zhao X, Chen P, Liu X, et al. Erratum to: ultra-high current gain tunneling hot-electron transfer amplifier based on vertical van der Waals heterojunctions. Nano Res, 2020, 13: 2308
8 Vaziri S, Lupina G, Henkel C, et al. A graphene-based hot electron transistor. Nano Lett, 2013, 13: 1435–1439
9 Al-Tabbakh A A, More M A, Joag D S, et al. The Fowler-Nordheim plot behavior and mechanism of field electron emission from ZnO tetrapod structures. ACS Nano, 2010, 4: 5585–5590